Available online at www.elixirpublishers.com (Elixir International Journal)

Computational Chemistry

Elixir Comp. Chem. 82A (2015) 32746-32753

ISSN: 2229-712X

Molecular and Vibrational Structure of 2,4-Difluoroanisole: FT-IR, FT-Raman, First-Order Hyperpolarizability, Electronic Excitation Mechanism and Quantum Chemical Calculations

M.K.Subramanian* and G.Adalarasu

Post Graduate and Research Department of Physics, Thiruvalluvar Government Arts College, Rasipuram, India.

ARTICLE INFO

Article history:

Received: 18 March 2015;

Received in revised form:

20 May 2015;

Accepted: 25 May 2015;

Keywords

Density Functional Theory,
FT-Raman,
FT-IR, FMO's
First-order Hyperpolarizability,
Electronic Excitation Energy.

ABSTRACT

The optimized molecular structure and corresponding vibrational assignments of 2,4-Difluoroanisole (24DFA) have been investigated using density functional theory (DFT)/B3LYP with 6-311+G** basis sets. The Fourier transform infrared and Fourier transform Raman spectra of title molecules were recorded. A detailed interpretation of the FT-IR and FT-Raman spectra of 24DFA are reported on the basis of the calculated potential energy distribution. The theoretically calculated harmonic frequencies are scaled by common scale factor. The observed and the calculated frequencies are found to be in good agreement. Frontier Molecular Orbitals (FMOs) have been constructed at B3LYP/6-311+G** level to understand the electronic properties. The first hyperpolarizability (β_0) of this noval molecular system and related properties (β, α_0, and $\Delta\alpha$) of 24DFA are calculated using B3LYP/6-311+G** method on the finite-field approach. Finally the calculations results were applied to simulated infrared and Raman spectra of the title compound which show good agreement with observed spectra. The chemical parameters were calculated from the HOMO and LUMO values. Electronic excitation energies, oscillator strength and nature of the respective excited states were calculated by the closed-shell singlet calculation method were also calculated for the molecule.

Introduction

Anisole is a solvent used in the synthesis of organic compounds and in large-scale applications such as the production of perfumes. Anisole has been used directly in the synthesis of the marine pyrrole alkaloids. Anisole may also be utilized in the preparation of inorganic complexes and materials, such as tin-core/tin oxide nanoparticles. Anisole is frequently used in the solid-phase synthesis of compounds, particularly in the cleavage of compounds from the resin. Modern vibrational spectroscopy has proven to be an exceptionally powerful technique for solving many chemistry problems. It has been extensively employed both in the study of chemical kinetics and chemical analysis.

In the present study, we extend the probing into the application of the B3LYP/6-311+G** based on SQM method to vibrational analysis and the energy calculations. The geometrical parameters of the most optimized geometry of 2,4-difluoroanisole [24DFA] obtained via energy calculations were used for the DFT calculations. The Infrared and Raman intensities were also predicted, based on these calculations, the simulated FTIR and FT-Raman spectra were obtained. The observed and the simulated spectra agree well. Further, density functional theory (DFT) combined with quantum chemical calculations to determine the first-order hyperpolarizability. The calculated HOMO and LUMO energies shows that charge transfer occur within the molecule. Electronic excitation energies, oscillator strength and nature of the respective excited states were calculated by the closed-shell singlet calculation method were also calculated for the molecule.

Experimental Details

The compound 24DFA was purchased from the Sigma–Aldrich Chemical Company (USA) with a stated purity of greater than 98% and it was used as such without further purification. The FT-Raman spectrum of 24DFA has been recorded using 1064 nm line of Nd:YAG laser as excitation wavelength in the region 4000-100 cm^{-1} on a Brucker model IFS 66V spectrophotometer equipped with FRA 106 FT-Raman module accessory. The FT-IR spectrum of this compound was recorded in the region 4000–400 cm^{-1} on IFS 66V spectrophotometer.

Computational Details

Quantum chemical methods based on density functional theory are now widely used for calculations of the structure and vibrational frequencies of molecules [1]. The molecular geometry optimizations, energy and vibrational frequency calculations were carried out for 24DFA with the GAUSSIAN 09W software package [2] using the B3LYP functionals [3,4] combined with the standard 6-31G* and 6-311+G** basis sets. The Cartesian representation of the theoretical force constants have been computed at optimized geometry by assuming C_s point group symmetry. Scaling of the force field was performed according to SQM procedure [5] using selective scaling in the natural internal coordinate representation [6,7]. Transformations of the force field and the subsequent normal coordinate analysis including the least square refinement of the scaling factors, calculation of the potential energy distribution (PED) and the prediction of IR and Raman intensities were done on a PC with the MOLVIB program written by Sundius [8].

To achieve close agreement between the observed and calculated frequencies, the least square fit refinement algorithm was used. The force field obtained this way was then used to recalculate the normal modes, PED's and the corresponding

Tele:
E-mail addresses: profdrmks@gmail.com

theoretically expected IR and Raman intensities to predict the full IR and Raman spectra.

The Raman activities (Si) calculated with the GAUSSIAN 09W program and adjusted during the scaling procedure with MOLVIB were subsequently converted to relative Raman intensities (Ii) using the following relationship derived from the basic theory of Raman scattering [9-10].

$$I_i = \frac{f(v_o - v_i)^4 S_i}{v_i[1-\exp(-hcv_i / KT)} \text{ ----------(1)}$$

Where υ_0 is the exciting frequency (in cm^{-1}), υ_i is the vibrational wavenumber of the i^{th} normal mode; h, c and k are fundamental constants, and f is a suitably chosen common normalization factor for all peak intensities.

Results and discussion

Molecular geometry

The molecular structure of 24DFA is shown in Fig 1. The global minimum energy obtained by the DFT structure optimization for the title compound is presented in Table 1. The bond length, bond angle and dihedral angles determined at the DFT level of theory for the 24DFA compound are listed in Table 2.

The geometrical optimization studies of 24DFA reveal that the molecule belongs to C_s symmetry point group. Detailed descriptions of vibrational modes can be given by means of normal coordinate analysis. For this purpose, the full set of 55 standard internal coordinates containing 13 redundancies for 24DFA was defined as given in Table 3. From there non redundant set of local symmetry coordinates was constructed by suitable liner combinations of internal coordinates following the recommendations of Fogarasi and Pulay [6] is presented in Table 5.4. The theoretically calculated DFT force fields were transformed in this later set of vibrational coordinates and used in all subsequent calculations.

Vibrational analysis

The 42 normal modes of 24DFA are distributed among the symmetry species as Γ_{3N-6}= 29 A' (in-plane) + 13 A″ (out-of-plane), and in agreement with C_s symmetry. All the vibrations were active both in Raman scattering and Infrared absorption.

The calculated frequencies of 24DFA compared with observed frequencies by normal mode analysis based on scaled quantum mechanical force field calculations are depicted in Table 5. For visual comparison, the observed and simulated FT-IR and FT-Raman spectra of 24DFA are produced in a common frequency scales in Fig 2 & Fig 3.

Root mean square (RMS) values of frequencies were obtained in the study using the following expression,

$$RMS = \sqrt{\frac{1}{n-1}\sum_{i}^{n}\left(\upsilon_i^{calc} - \upsilon_i^{exp}\right)^2}$$

In order to reproduce the observed frequencies, refinement of scaling factors were applied and optimized via least square refinement algorithm which resulted a weighted RMS deviation from 116 cm^{-1} to 7.02 cm^{-1} for the B3LYP/ 6-311+G** basis sets, respectively, between experimental and SQM frequencies. The good agreement allows us to perform the assignments of the IR and Raman bands to the normal modes in the whole studied spectral regions. From high to low wave number the following comments are in order.

C–H vibrations

The Infrared bands at 3247, 3245, 3242, 3212, 3210 and 3209 cm^{-1} are assigned to C–H stretching vibrations and FT-Raman bands at 3222, 3220 and 3218 cm^{-1} were assigned to in-plane bending vibration [11]. The C–H out of plane bending vibration are observed at 855, 852, 850, 834, 831 and 829 cm^{-1} for the 24DFA compound was well identified in the recorded spectra, within their characteristic region.

C-C vibrations

The highest C–C stretching vibration is around 1700-1600 cm^{-1}. The vibrations should appear near 1700-1600 cm^{-1} giving rise to a fairly strong bands IR and Raman spectra. In present investigation, the C-C mode mixes with C–H in-plane bending vibrations. The IR and Raman bands observed at 1683, 1682, 1678 cm^{-1} and 1657, 1655, 1653 cm^{-1} respectively.

Ring vibrations

Several ring modes are affected by the substitution to the aromatic ring of 24DFA. In the present study, the bands ascribed at 946, 945, 942, 855, 852, 850, 746, 745 and 740 cm^{-1} for 24DFA have been designated to ring in-plane and out-of plane bending modes, respectively. The reduction in frequencies of these modes compared to 24DFA is due to the changes in the force constant, resulting mainly from addition of CF, CO and from different extents of mixing between the ring and substituent groups vibration.

C–F vibrations

In 24DFA, the C–F stretching and in-plane bending vibrations appeared at 1358, 1356, 1354, 1292, 1289, 1287 and 1286 cm^{-1} respectively in IR and Raman. The C–F out of-plane bending vibration was found at 855, 852, 850 and 834, 831, 829 cm^{-1} in IR and Raman spectrum.

C–O vibrations

The bands observed at 1566, 1565, 1562, 1358, 1356 and 1354 cm^{-1} in C–O stretching vibrations for the 24DFA compound. This mode can be described as vibrations, involving main contributions from the C-O stretching vibrations [12]. The C-O out-of-plane vibration has an important contribution to Table 5.5. These modes are strongly coupled with ring torsion modes also.

Methyl group vibrations

The 24DFA compound, under consideration possesses only one CH_3 group in the ring, respectively. For the assignments of CH_3 group frequencies, one can expect that nine fundamentals can be associated to each CH_3 group, namely the symmetrical (CH_3 ips) and asymmetrical (CH_3 ops), inplane stretching modes (i.e. in-plane hydrogen stretching mode); the symmetrical (CH_3 ss), and asymmetrical (CH_3 ips), deformation modes; the in-plane rocking (CH_3 ipr) out-of-plane rocking (CH_3 opr) and twisting (t CH_3) bending modes. In addition to that, the asymmetric stretching (CH_3 ops) and asymmetric deformation (CH_3 opb) modes of the CH_3 group are expected to be depolarised for A'' symmetry species. In the present work, the frequencies observed in the FT-Raman and FT-IR spectrum at 3197, 3195, 3193 and 3129, 3126, 3125 cm^{-1} have been assigned to CH_3 ss, CH_3 ips and CH_3 ops stretching vibrations. The CH_3 in-plane bending vibrations of the 24DFA are well indentified at 1219, 1215 and 1212 cm^{-1} in the FT-IR spectra which are found to be well within their characteristic region.

First-order hyperpolarizability calculations

The first-order hyperpolarizibility (β_{ijk}) of the novel molecular system of 24DFA is calculated using B3LYP/6-311+G** basis set based on finite field approach. Hyperpolarizibility is a third rank tensor that can be described by a 3 x 3 x 3 matrix. It strongly depends on the method and basis set used. The 27 components of 3D matrix can be reduced to 10 components due to Kleinman [13] symmetry. The calculated first-order hyperpolarizability (β_{total}) of 24DFA is

95.734x10^{-30} esu, which is greater than that of urea (0.1947x 10^{-30} esu). The calculated dipole moment (μ) and first-order hyperpolarizibility (β) are shown in Table 6.

Frontier Molecular Orbitals (FMO)

The highest occupied molecular orbital (HOMO) and lowest–lying unoccupied molecular orbital (LUMO), called frontier molecular orbitals (FMO) are the most important orbitals in a molecule. FMOs play important roles in interaction between the molecules as well as electron spectra of molecule [14]. The energy gap between HOMO and LUMO determines the chemical reactivity, kinetic stability, optical polarizability and chemical hardness-softness of a molecule. The chemical hardness is a good indicator of the chemical stability. The molecules having large energy gap are known as hard and having a small energy gap are known as soft molecules. The hardness value of the molecule is formulated by the following equation [15].

$$\eta = (-\varepsilon_{HOMO}+\varepsilon_{LUMO}) / 2$$

where ε_{HOMO} and ε_{LUMO} are the energies of the HOMO and LUMO orbitals.

The chemical hardness value is 0.007 a.u. for the title molecule. Moreover, the lower value in the HOMO and LUMO energy gap explains the eventual charge transfer interactions taking place within the molecule.

Electronic excitation energies, oscillator strength and nature of the respective excited states were calculated by the closed-shell singlet calculation method and are summarized in Table 7. Fig 4 shows the highest occupied molecule orbital (HOMO) and lowest unoccupied molecule orbital (LUMO) of 24DFA. There is an inverse relationship between hyperpolarizability and HOMO–LUMO. The title molecule contains 75 molecular orbitals and Fig 4(a) and 4(b) shows the distribution and the energy level orbitals for the molecule in gas phase. It is clear from the figure that the HOMO and LUMO orbitals are mainly delocalized over the molecules. Orbital involved in the electronic transition for (a) HOMO−0 (b) LUMO+0 (c) HOMO-1 (d) LUMO+1 (e) LUMO+2 is represented in Fig 5.

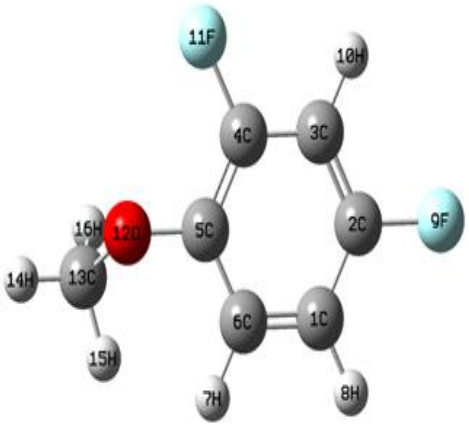

Fig 1. The optimized molecular structure of 24DFA

LUMO as an electron acceptor represents the ability to obtain an electron, HOMO represents the ability to donoate an electron.

HOMO energy = -0.013 a.u

LUMO energy = 0.001 a.u

HOMO–LUMO energy gap = 0.014 a.u

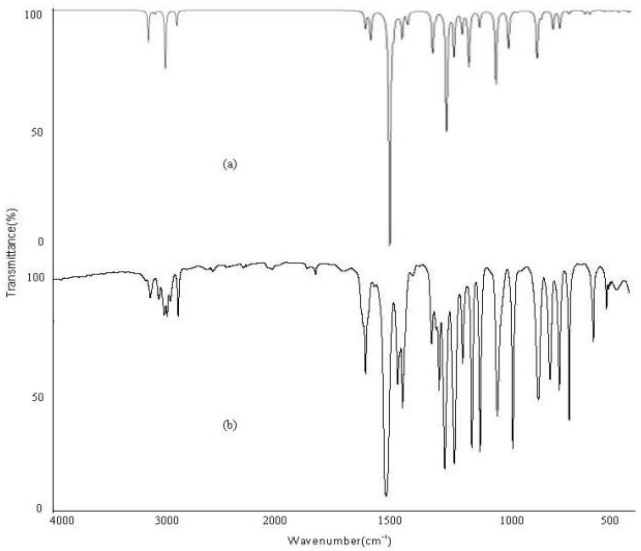

Fig 2. FT-IR spectra of 24DFA
(a)Calculated (b) Observed with B3LYP/6-311+G**

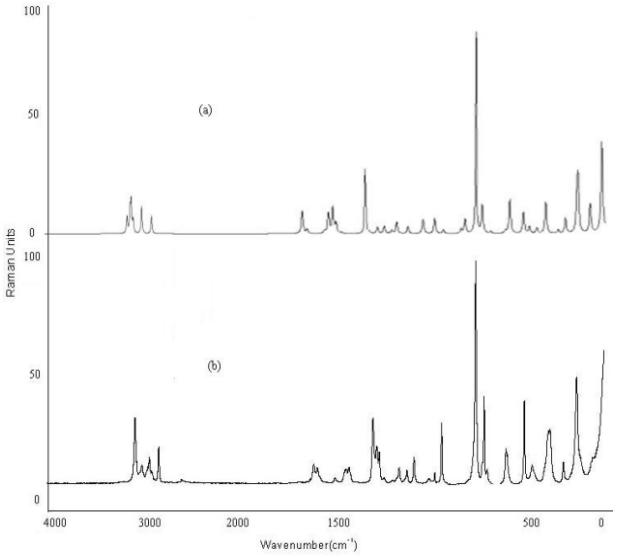

Fig 3. FT-Raman spectra of 24DFA
(a) Calculated (b) Observed with B3LYP/6-311+G**

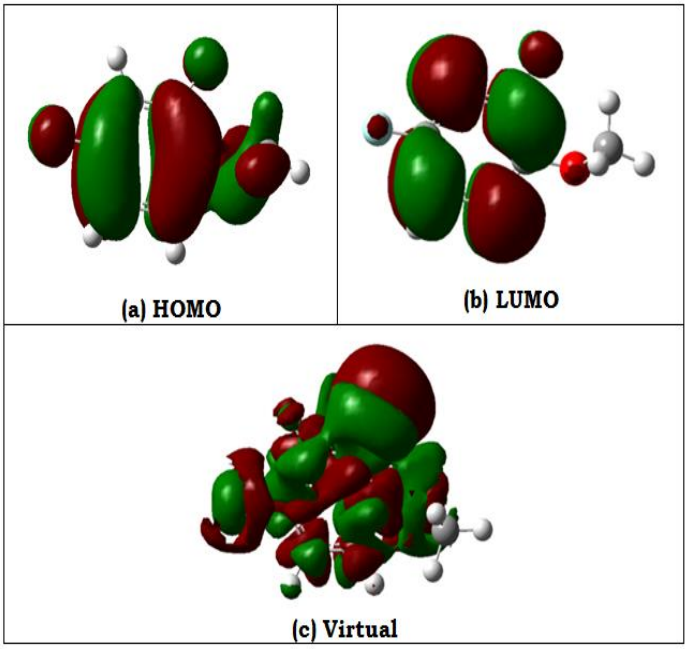

Fig 4. Representation of the orbital involved in the electronic transition for (a) HOMO (b) LUMO (c) Virtual

Table 1. Total energies of 24DFA, calculated at DFT B3LYP/6-31G* and B3LYP/6-311+G level**

Method	Energies (Hartrees)
6-31G*	-545.22654100
6-311+G**	-545.23016135

Table 2. Optimized geometrical parameters of 24DFA obtained by B3LYP/6–311+G density functional calculations**

Bond length	Value(Å)	Bond angle	Value(Å)	Dihedral angle	Value(Å)
C2-C1	1.38607	C3-C2-C1	120.00160	C4-C3-C2-C1	0.00000
C3-C2	1.38599	C4-C3-C2	120.00023	C5-C4-C3-C2	0.00000
C4-C3	1.38600	C5-C4-C3	120.00023	C6-C1-C2-C3	0.00000
C5-C4	1.38599	C6-C1-C2	119.99816	H7-C6-C1-C2	-179.42800
C6-C1	1.38600	H7-C6-C1	119.99639	H8-C1-C6-C5	179.42805
H7-C6	1.12192	H8-C1-C6	120.00081	F9-C2-C1-C6	179.42724
H8-C1	1.12197	F9-C2-C1	119.99692	H10-C3-C2-C1	179.42803
F9-C2	1.49005	H10-C3-C2	119.99647	F11-C4-C3-C2	179.42719
H10-C3	1.12197	F11-C4-C3	119.99692	O12-C5-C4-C3	-179.42753
F11-C4	1.48993	O12-C5-C4	119.99899	C13-O12-C5-C4	120.00249
O12-C5	1.40995	C13-O12-C5	109.49805	H14-C13-O12-C5	180.00000
C13-O12	1.41007	H14-C13-O12	109.49766	H15-C13-O12-C5	59.93400
H14-C13	1.12204	H15-C13-O12	109.50118	H16-C13-O12-C5	-59.93415
H15-C13	1.12193	H16-C13-O12	109.49953		
H16-C13	1.12193				

*for numbering of atom refer Fig 1

Table 3. Definition of internal coordinates of 24DFA

No(i)	symbol	Type	Definition
Stretching 1-6	r_i	C-C	C1-C2,C2-C3,C3-C4,C4-C5,C5-C6,C6-C1
7-9	S_i	C-H	C1-H8,C3-H10,C6-H7
10-11	p_i	C-F	C2-F9,C4-F11
12-13	P_i	C-O	C5-O12,C13-O12
14-16	ψ_i	C-H(m)	C13-H14,C13-H15,C13-H16
Bending 17-22	α_i	C-C-C	C1-C2-C3,C2-C3-C4,C3-C4-C5, C4-C5-C6,C5-C6-C1,C6-C1-C2
23-28	θ_i	C-C-H	C5-C6-H7, C1-C6-H7,C6-C1-H8, C2-C1-H8, C2-C3-H10, C4-C3-H10
29-32	β_i	C-C-F	C1-C2-F9, C3-C2-F9,C3-C4-F11, C5-C4-F11
33-34	Φ_i	C-C-O	C4-C5-O12, C6-C5-O12
35	γ_i	C-O-C	C5-O12-C13
36-38	ε_i	H-C-H	H14-C13-H15, H15-C13-H16, H16-C13-H14
39-41	ι_i	C-O-C	O12-C13-H14,O12-C13-H15, O12-C13-H16
Out-of-plane 42-44	ω_i	C-H	H7-C6-C5-C1,H8-C1-C2-C6, H10-C3-C4-C2
45	ξ_i	C-O	O12-C5-C4-C6
46-47	Ω_i	C-F	F9-C2-C1-C3, F11-C4-C5-C3
Torsion 48-53	τ_i	C-C	C1-C2-C3-C4,C2-C3-C4-C5, C3-C4-C5-C6,C4-C5-C6-C1, C5-C6-C1-C2,C6-C1-C2,C3
54	τ_i	C-O	C4(C6)-C5-O12-C13
55	τ_i	C-O-H	C5-O12-C13-(H14,H15,H16)

*for numbering of atom refer Fig 1

Table 4. Definition of local symmetry coordinates and the value corresponding scale factors used to correct the force fields for 24DFA

No.(i)	Symbol[a]	Definition[b]	Scale factors used in calculation
1-6	C-C	r1,r2,r3,r4,r5,r6	0.914
7-9	C-H	S7,S8,S9	0.914
10-11	C-F	p10,p11	0.992
12-13	C-O	P12,P13	0.992
14	mss	(ψ14+ψ15+ψ16)/ √3	0.995
15	mips	(2ψ15-ψ14-ψ16)/ √6	0.992
16	mops	(ψ15-ψ16)/ √2	0.919
17	C-C-C	(α17-α18+α19-α20+α21-α22)/ √6	0.992
18	C-C-C	(2α17-α18-α19+2α20-α21-α22)/ √12	0.992
19	C-C-C	(α18-α19+α21-α22)/2	0.992
20-22	C-C-H	(θ23-θ24)/√2,(θ25-θ26)/√2, (θ27-θ28)/√2	0.916
23-24	C-C-F	(β29-β30)/√2, (β31-β32)/√2	0.923
25	C-C-O	(Φ33- Φ34)/√2	0.923
26	C-O-C	γ35	0.990
27	msb	(ε36+ε37+ε38-ι39-ι40-ι41)/ √6	0.990
28	mipb	(2ε38-ε36-ε37)/ √6	0.990
29	mopb	(ε36-ε38)/ √2	0.990
30	mipr	(2ι40-ι39-ι41)/ √6	0.990
31	mopr	(ι39-ι41)/ √2	0.990
32-34	C-H	ω42, ω43, ω44	0.994
35	C-O	ξ45	0.962
36-37	C-F	Ω46, Ω47	0.962
38	tring	(τ48-τ49τ50-τ51+τ52-τ53)/√6	0.994
39	tring	(τ48-τ50+τ51-τ53)/2	0.994
40	tring	(-τ48+2τ49-τ50-τ51+2τ52-τ53)/√12	0.994
41	C-O	τ54	0.979
42	C-O-H	τ55/3	0.979

[a] These symbols are used for description of the normal modes by TED in Table 5.
[b] The internal coordinates used here are defined in Table 3.

Table 5. Detailed assignments of fundamental vibrations of 24DFA by normal mode analysis based on SQM force field calculation

S. No.	Symmetry species C_s	Observed frequency (cm^{-1})		Calculated frequency (cm^{-1}) with B3LYP/6-311+G ** force field				TED (%) among type of internal coordinates[c]
		Infrared	Raman	Unscaled	Scaled	IR[a] A_i	Raman[b] I_i	
1	A'	3247		3245	3242	35.013	77.571	CH(99)
2	A'		3222	3220	3218	0.046	107.572	CH(99)
3	A'	3210		3212	3209	2.101	138.764	CH(99)
4	A'		3197	3195	3193	3.670	57.030	mops(91),mips(6)
5	A'	3129		3126	3125	63.866	115.602	mips(78),mss(12),mops(9)
6	A'			3049	3046	16.915	69.511	mss(84),mips(15)
7	A'	1683		1682	1678	18.774	22.599	CC(65),bCH(14),bring(12)
8	A'		1657	1655	1653	31.102	4.017	CC(74),bring(10),bCH(5)
9	A'	1566		1565	1562	269.104	2.219	CC(38),bCH(30),CO(11),CF(10),bmsb(6)
10	A'			1544	1542	18.170	17.230	bmipb(81),bmopb(14)
11	A'		1524	1522	1519	2.502	21.563	bmopb(64),bmipb(33)
12	A'	1510		1506	1502	29.095	8.162	bmsb(65),bmopb(12),CC(9),bCH(5)
13	A'			1478	1475	14.425	0.901	CC(44),bCH(15),CF(14),bmsb(12),bCF(7)
14	A'		1358	1356	1354	45.640	9.596	CC(58),CF(19),CO(10),bCH(8)
15	A'			1342	1339	4.621	7.362	CC(80),CF(7),CO(5)
16	A'	1286	1292	1289	1287	131.513	4.062	bCH(46),CO(23),bring(11),CF(9)
17	A'			1254	1251	47.580	4.545	bCH(23),bmopr(19),CO(14),bring(10),CF(8),bmipr(8)
18	A'	1219	1217	1215	1212	24.187	1.766	bmopr(41),bmipr(14),bCH(14),bring(8),CO(8),CC(7)
19	A'			1189	1186	0.394	6.048	bmipr(49),bmopr(18),bmopb(12),bmipb(9),bCH(5)
20	A'	1183		1182	1179	60.483	0.434	bCH(39),CF(36),bmipr(8),CC(7)
21	A'		1129	1131	1127	18.399	3.579	bCH(51),CC(21),bring(10),CF(10)
22	A'	1054		1052	1048	79.963	6.260	CO(77),bring(9),CC(7)
23	A'			991	988	41.601	6.458	CC(37),CF(21),bring(20),bCH(16)
24	A"		946	945	942	1.792	1.420	gCH(87),tring(11)
25	A"	855		852	850	52.879	1.368	gCH(73),tring(16),gCF(10)
26	A"		834	831	829	6.485	4.532	gCH(71),tring(14),gCO(7),gCF(6)
27	A'			775	773	20.429	17.624	CC(33),CO(26),bring(18)
28	A'	746		745	740	19.556	7.435	bring(43),CF(17),CC(11),CO(6),tring(6)
29	A"		698	697	695	3.556	0.511	tring(53),gCF(21),gCO(17)
30	A"			620	618	3.779	0.538	gCF(46),tring(45)
31	A'	597		598	595	4.045	6.672	bCO(27),bCF(24),bring(16),CC(12),gCF(7)
32	A'		529	528	525	1.116	3.516	bring(34),gCF(17),tring(14),bCOC(9),bCF(7),CC(7)
33	A"	498		496	493	0.960	1.004	tring(33),gCF(28),bCF(12),bring(8),gCO(7),bCOC(6)
34	A"		457	459	455	1.971	0.748	tring(45),bring(17),gCF(11),gCH(8),bCF(7)
35	A"	414		412	409	2.157	3.538	tring(31),bring(26),gCH(11),gCF(10),bCOC(6)
36	A'			346	343	4.150	0.321	bCF(49),bCO(18),CC(13)
37	A'		302	309	305	0.028	1.120	bCF(38),bCO(18),gCO(11),bCOC(10),bring(7),tring(6)
38	A"			248	245	3.527	1.569	tring(35),bCO(20),bCOC(16),gCO(13)
39	A"		247	245	240	0.922	2.236	tring(37),gCF(23),gCH(21),bCO(7),bCOC(5)
40	A"			179	176	1.991	0.846	tOCH3(54),tring(23),tCOm(14)
41	A"		118	120	116	0.406	1.247	tring(49),tOCH3(15),gCO(12),gCH(9),tCOm(6)
42	A"			55	50	3.417	1.037	tCOm(60),bCO(14),bCOC(11),tOCH3(9)

Abbreviations used: b, bending; g, wagging; t, torsion; s, strong; vs, very strong; w, weak; vw, very weak;

[a] Relative absorption intensities normalized with highest peak absorption

[b] Relative Raman intensities calculated by Eq 1 and normalized to 100.

[c] For the notations used see Table 4.

Table 6. The dipole moment (μ) and first-order hyperpolarizibility (β) of 24DFA derived from DFT calculations

β_{xxx}	**-23.236**
β_{xxy}	-380.87
β_{xyy}	953.21
β_{yyy}	-31.091
β_{zxx}	-55.451
β_{xyz}	401.54
β_{zyy}	-8449.6
β_{xzz}	-920.33
β_{yzz}	-10.533
β_{zzz}	-25.558
β_{total}	95.734
μ_x	0.09339112
μ_y	0.29625204
μ_z	1.31146976
μ	1.30426719

Dipole moment (μ) in Debye, hyperpolarizibility $\beta(-2\omega;\omega,\omega)$ 10^{-30}esu.

Table 7. Computed absorption wavelength (λ_{ng}) , energy (E_{ng}), oscillator strength (f_n) and its major contribution

n	λ_{ng}	E_{ng}	f_n	Major contribution
1	193.8	6.40	0.0222	H-0->L+0(+64%), H-1->L+1(+33%)
2	186.5	6.65	0.0022	H-0->L+1(+48%), H-1->L+0(47%)
3	160.4	7.73	0.0011	H-0->L+2(+71%)

(Assignment; H=HOMO,L=LUMO,L+1=LUMO+1,etc.)

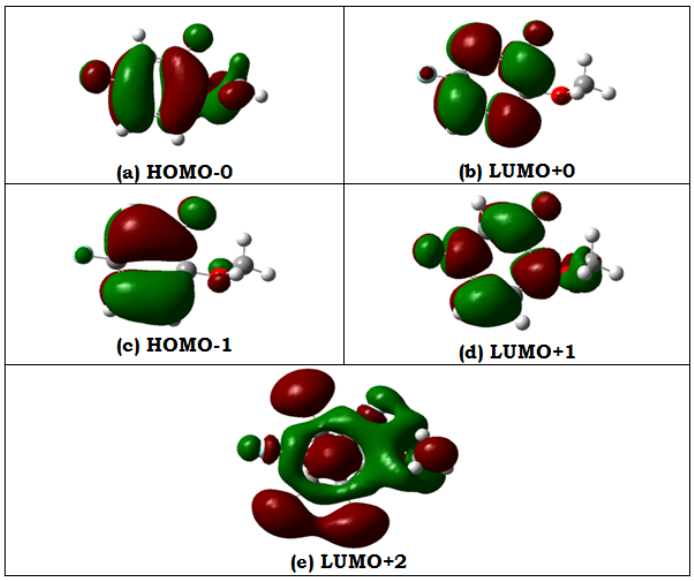

Fig 5. Representation of the orbital involved in the electronic transition for (a) HOMO−0 (b) LUMO+0 (c) HOMO-1 (d) LUMO+1 (e) LUMO+2

Conclusions

In this work, the SQM force field method based on DFT calculations at the B3LYP/6-311+G** level have been carried to analyze the vibrational frequencies of 24DFA. Refinement of scaling factors were applied and optimized via least square refinement algorithm which resulted a weighted RMS deviation from 116 cm^{-1} to 7.02 cm^{-1} for the B3LYP/6-311+G** basis sets. This close agreement established between the experimental and scaled frequencies obtained using large basis set B3LYP/6-311+G** calculations have proved to be more reliable and accurate than the calculations using lower basis sets. The first-order hyperpolarizibility (β_{ijk}) of the novel molecular system of 24DFA is calculated using B3LYP/6-311+G** basis set based on finite field approach. The calculated first-order hyperpolarizability (β_{total}) of 24DFA is 95.734x10^{-30} esu, which is greater than that of urea (0.1947x10^{-30} esu). Electronic excitation energies, oscillator strength and nature of the respective excited states were calculated by the closed-shell singlet calculation method. The chemical hardness value is 0.007 a.u. for the title molecule. Moreover, the lower value in the HOMO and LUMO energy gap explains the eventual charge transfer interactions taking place within the molecule. The HOMO and LUMO orbitals are mainly delocalized over the molecules.

References

1. G. Rauhut, P. Pulay, J. Phys. Chem. 99 (1995) 3093.
2. M. J. Frisch, G. W. Trucks, H. B. Schlegel, G. E. Scuseria, M. A. Robb, J. R. Cheeseman, G. Scalmani, V. Barone, B. Mennucci, G. A. Petersson, H. Nakatsuji, M. Caricato, X. Li, H. P. Hratchian, A. F. Izmaylov, J. Bloino, G. Zheng, J. L. Sonnenberg, M. Hada, M. Ehara, K. Toyota, R. Fukuda, J. Hasegawa, M. Ishida, T. Nakajima, Y. Honda, O. Kitao, H. Nakai, T. Vreven, J. A. Montgomery, Jr., J. E. Peralta, F. Ogliaro, M. Bearpark, J. J. Heyd, E. Brothers, K. N. Kudin, V. N. Staroverov, R. Kobayashi, J. Normand, K. Raghavachari, A. Rendell, J. C. Burant, S. S. Iyengar, J. Tomasi, M. Cossi, N. Rega, J. M. Millam, M. Klene, J. E. Knox, J. B. Cross, V. Bakken, C. Adamo, J. Jaramillo, R. Gomperts, R. E. Stratmann, O. Yazyev, A. J. Austin, R. Cammi, C. Pomelli, J. W. Ochterski, R. L. Martin, K. Morokuma, V. G. Zakrzewski, G. A. Voth, P. Salvador, J. J. Dannenberg, S. Dapprich, A. D. Daniels, O. Farkas, J. B. Foresman, J. V. Ortiz, J. Cioslowski, and D. J. Fox, Gaussian, Inc., Wallingford CT, 2009.
3. A.D. Becke, J. Chem. Phys., 98 (1993) 5648.
4. C. Lee, W. Yang, R.G. Parr, Phys. Rev., B37 (1988) 785.
5. G.W. King, Spectroscopy and Molecular Structure, Rinehart and Winsten, Inc., New York, 1964.
6. G. Foragarasi, P. Pulay, in: J.R. Durig (Ed.), Vibrational Spectra and Structure, vol. 14, Elsevier, Amsterdam, 1985, pp. 125–219.

7. P. Pulay, in: H.F. Schaefer III (Ed.), Application of Electronic structure Theory, Modern Theoretical Chemistry, vol. 4, Plenum press, New York, 1997, p. 153.
8. V. Krishnakumar, Gabor Keresztury, Tom Sundius, S. Seshadri, Spectrochimica Acta Part A: Molecular and Biomolecular Spectroscopy, Volume 68, Issue 3, November 2007, Pages 845-850.
9. G. Keresztury, S. Holly, J. Varga, G. Besenyei, A.Y. Wang, J.R. Durig, Spectrochim. Acta 49A (1993) 2007.
10. G. Keresztury, in: J.M. Chalmers, P.R. Griffiths (Eds.), Raman Spectroscopy: Theory in Handbook of Vibrational Spectroscopy, vol.1, John Wiley & Sons Ltd., 2002.
11. A. Suvitha, S. Periandy and P. Gayathri, Spectrochimica Acta Part A: Molecular and Biomolecular Spectroscopy, 138 (2015) 357-369.
12. Yaping Tao, Ligang Han, Yunxia Han and Zhaojun Liu, Spectrochimica Acta Part A: Molecular and Biomolecular Spectroscopy, 137 (2015) 1078-1085.
13. D.A. Kleinman, Phys. Rev. 1962;126,1977.
14. O. Prasad, L,sinha, N. Misra,V.Narayan, N.Kumar, J.Pathak, J. Mol. Struct. Theochem. 940 (2010)82-86.
15. R.G.Pearson, Proc. Natl.Acad. Sci. 83 (1986) 8440-8841.